

STYRELSEN FÖR  
**VINTERSJÖFARTSFORSKNING**  
WINTER NAVIGATION RESEARCH BOARD

Research Report No 131

Hanyang Gong

**A REVIEW OF NUMERICAL METHODS FOR  
ESTIMATING SHIP RESISTANCE IN FSICR CHANNEL**

Finnish Transport and Communications Agency

Finnish Transport Infrastructure Agency

Finland

Swedish Maritime Administration

Swedish Transport Agency

Sweden

Talvimerenkulun tutkimusraportit — Winter Navigation Research Reports  
ISSN 2342-4303  
ISBN 978-952-311-908-6

## FOREWORD

In this report no 131, the Winter Navigation Research Board presents the results of a research project on a review of numerical methods for estimating ship resistance in FSICR channel. The project investigates different publicly available simulation tools for estimating ship resistance in ice channel that might in the future allow alternative ways to estimate ship resistance in Finnish-Swedish Ice Class Rules.

The Winter Navigation Research Board warmly thanks Hanyang Gong for this report.

Helsinki

March 2024

Ville Häyrynen

Finnish Transport and Communications Agency

Amund Lindberg

Swedish Maritime Administration

Helena Orädd

Finnish Transport Infrastructure Agency

Fredrik Hellsberg

Swedish Transport Agency

**AKER ARCTIC TECHNOLOGY INC REPORT**

**A REVIEW OF NUMERICAL METHODS FOR  
ESTIMATING SHIP RESISTANCE IN FSICR  
CHANNEL**

**FOR**

**FINNISH TRANSPORT AND  
COMMUNICATIONS AGENCY**

<b>Name of document:</b> A review of numerical methods for estimating ship resistance in FSICR channel			
<b>Document Responsible:</b> Hanyang Gong		<b>Document Co-Author(s):</b>	
<b>Document Reviewer:</b> Riikka Matala		<b>Document Approver:</b> Topi Leiviskä	
<b>Report number / Revision:</b> K544 / A		<b>Status / Status Date:</b> Approved / 2023-12-20	
<b>Client:</b> Finnish Transport and Communications Agency / Ville Häyrynen			
<b>Revision remarks:</b>			
<p>Ice-going merchant ships have been designed to be customised for operating in ice and open water. Merchant ships operating in the Baltic Sea are required to be classified based on the Finnish-Swedish Ice Class Rules (FSICR) to operate at a minimum of 5 knots in an ice class brash ice channel. The performance can be verified by ice model tests. As merchant ships may perform at a relatively high speed in brash ice, the current model tests may face challenges from the effect of hydrodynamics on the brash icebreaking process. In addition, some modern bow forms experience significant resistance by displacing brash ice mass sideways, which has not been realistically modelled with the current Froude-Cauchy scaling approach. Numerical simulations as alternatives for calculating ice resistance have shown their potential to assist model tests on ice performance prediction.</p> <p>This review supports the work for future numerical method development. It first reviews previous studies on numerically simulating ships in a brash ice channel. A brash ice channel is a particle-fluid system. To the current knowledge, the discrete element method (DEM) of simulating brash ice has become outstanding among other numerical methods, such as the finite element method, smoothed particle hydrodynamics, physics engine, etc. Recently, studies of coupling computational fluid mechanics (CFD) with DEM for brash ice channel simulation have mainly utilised commercial simulation software STAR-CCM+ by using the integrated contact models in the software. Therefore, it is worth developing a numerical simulation model using an open-source DEM-CFD platform with the possibility of custom user settings on the contact models. This report presents the techniques of DEM, CFD, and coupling methods. Two potential open-source DEM-CFD simulation platforms with two-way coupling could be launched to apply ships in a brash ice channel by utilising parallel calculations. Some discussions are carried out by explicitly considering the first launch of the future work. The future DEM-CFD numerical tool will benefit the digitalisation of the winter navigation system. It can accurately predict ice performance in the brash ice channel for all types of ship hull forms by considering the effect of hydrodynamics alongside model tests. The ice load magnitude and distribution on the hull form can also be obtained.</p>			
<b>Keywords:</b> CFE; DEM; Coupling; Numerical methods; Brash ice resistance; Ice load.			
<b>Client reference:</b> PA (30941) - Finnish Transport and Communications Agency - WNRB W23-6 CresSi		<b>Project number:</b> 30941	<b>Language:</b> English
<b>Pages, total:</b> 27	<b>Attachments:</b> -	<b>Distribution list:</b> Client	<b>Confidentiality:</b> Confidential

## TABLE OF CONTENTS

- 1 INTRODUCTION .....5
- 1.1 BRASH ICE CHANNEL .....5
- 1.2 ICE CLASS SHIPS AND MODEL TEST .....7
- 1.3 SCOPE OF THIS REPORT .....7
- 2 NUMERICAL METHODS OF BRASH ICE .....8
- 2.1 DISCRETE ELEMENT METHOD (DEM) .....8
- 2.2 OTHER NUMERICAL METHODS .....11
- 2.2.1 OPEN DYNAMICS ENGINE .....11
- 2.2.2 FINITE ELEMENT METHOD COUPLED WITH ARBITRARY LAGRANGIAN EULERIAN .....11
- 2.2.3 SMOOTHED PARTICLE HYDRODYNAMICS .....12
- 3 CFD-DEM NUMERICAL METHOD OF SHIP IN BRASH ICE .....13
- 3.1 TECHNIQUES OF DEM .....14
- 3.1.1 GEOMETRY OF DISCRETE ELEMENTS .....14
- 3.1.2 CONTACT DETECTION .....15
- 3.1.3 PARTICLE MOTION EQUATION .....15
- 3.1.4 CONTACT FORCE .....16
- 3.1.5 PARTICLE-FLUID INTERACTION FORCE .....16
- 3.2 THEORY BACKGROUND OF CFD .....17
- 3.3 COUPLING SCHEME BETWEEN CFD AND DEM .....18
- 4 DISCUSSION .....21
- 5 CONCLUSION .....22
- 6 ACKNOWLEDGEMENT .....23
- REFERENCES .....24

## LIST OF FIGURES

- Figure 1: (a) Brash ice in a fairway channel in the Baltic Sea (Picture: Aker Arctic). (b) Vessel advancing in a brash ice channel and a transverse profile of a typical old brash ice channel in Baltic Sea. After Matala and Suominen (2023b) and Matala (2023).....6
- Figure 2: Laboratory scale (left) and virtual (right) punch through test on floating rubble. The colored lines describe the contours for rubble displacement. After Polojärvi (2013). ..9
- Figure 3: Ice blocks kinetic behaviour in an unconsolidated ice ridge passing by a ship, simulated by Aalto Ice Mechanics group in-house DEM after Gong et al. (2019a) and Gong (2021). .....9
- Figure 4: Force chains can be observed in ice ridge failure captured by DEM. After Gong et al. (2023).....10
- Figure 5: Ship in an ice floe field simulation by using the Aalto Ice Mechanics group’s in-house DEM code, after Polojärvi et al. (2021). .....10
- Figure 6: An ice-conical structure interaction simulation by Aalto Ice Mechanics group using in-house DEM after Polojärvi (2022). .....10

Figure 7: Snapshots of Japan Bulk Carrier navigation simulation in a brash ice channel. After Konno and Yoshida (2023) (left) and Tokudome and Konno (2023) (right)..... 11

Figure 8: Snapshots of the simulation (left) and the hull and ice interaction (right). After Kim et al. (2019)..... 12

Figure 9: Cylinder in brash ice using SPH with different material parameters. After Cabrera (2017). ..... 12

Figure 10: The view above the water of the experimental and numerical ship-ice interaction phenomenon. a. the side view of the interaction phenomena between ship hull and brash ice. After Luo, et al. (2022). ..... 13

Figure 11: A ship hull in cylinder particles channel simulated in STAR-CCM+. After Voutilainen (2022). ..... 14

Figure 12: Comparison between the model tests and simulation of a 108k bulk carrier in 1A FSICR brash ice channel. After Sun et al. (2023). ..... 14

Figure 13: Lethe CFD-DEM coupling scheme. After Geitani et al. (2023)..... 20

# 1 INTRODUCTION

Safe and effective shipping in ice-covered waters requires a reliable winter navigation system. In the Northern Baltic Sea area, the Finnish–Swedish winter navigation system governs maritime transportation in winter conditions, ensuring merchant vessels safely reach ports. Nowadays, ice-going merchant ships are typically designed to be customised for operating both in ice and open water. Merchant ships in the Baltic Sea are required to be classed based on the Finnish-Swedish Ice Class Rules (FSICR). The FSICR requires ships in each ice class to operate at a minimum of 5 knots in an ice class brash ice channel with a mid-part thickness specific for the ice class (1A – 1C).

Two rule methods are regulated in FSICR: semi-empirical calculation method and model test. The semi-empirical calculation method is limited by the empirical data of a limited number of traditional hull forms, not covering ship hulls with high stem angles.

In comparison, ice model tests could directly verify the ship's ice performance. As the merchant ships may perform at a relatively high speed in brash ice, the current model tests may face challenges from the effect of hydrodynamics on the brash icebreaking process. Recent work by Matala and Suominen (2022, 2023a) shows that the model test ice resistance seems to be overestimated compared with the full-scale measurements for certain bow forms. One reason is the scaled model brash ice used in the model tests. Using the Froude scaling law, the model brash ice would be too soft, which could not reflect the full-scale brash ice mechanical behaviour under the ship's passage. Using freshwater ice cubes instead of model brash ice to conduct the FSICR's brash ice channel tests has been recommended. By observing the brash ice movements during the tests, Matala and Suominen (2023b) also concluded that the ice displacement force dominates the resistance for certain bow shapes. Some modern bow forms experience significant resistance by displacing brash ice mass sideways, which has not been realistically modelled with the current Froude-Cauchy scaling approach.

Additionally, due to the current limitations of the model testing measurements, it is challenging to observe and study the brash ice failure behaviour on site. Therefore, alternative approaches are needed to evaluate the brash ice resistance and understand the brash ice failure behaviour under the ship's passage. Numerical simulations as alternatives for calculating ice resistance have shown their potential to assist model tests on ice performance prediction.

Before reviewing the numerical methods with the application on ships in the brash ice channel system, the introduction will shortly outline the brash ice channel definition and physical properties and the recent development of the ice-going ship hull forms to confine this study's objectives.

## 1.1 BRASH ICE CHANNEL

A brash ice channel is a primary ice condition for merchant ships in the winter navigation system in the Baltic Sea. Brash ice channels are typically opened by icebreakers along the fairway covered by ice, for instance, level ice, for merchant ships travelling between harbours. In the channel, the broken ice is called brash ice. Brash ice in the Baltic Sea



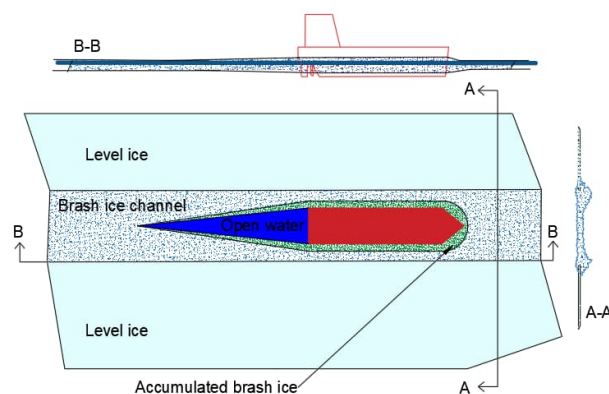
channels can appear in many forms. The properties are influenced by factors such as initial ice conditions, air temperature, and navigation frequency. For instance, in terms of shape and size, brash ice has different characters over time (new and old). The brash ice initial form is ice floe, freshly formed from level ice by the icebreaker's passage. As the channel is open, merchant ships start to travel in the channel, and the following passages break the floes smaller due to the ship-floe and floe-floe interactions. Combined with the repeated freezing cycles, the ice floes become smaller and rounder over time after multiple passages. At this stage, the ice floes in the channel are typically called old brash ice. As a result, the diameter of brash ice fragments seldom exceeds 1.0 m in the fairway channels of the Baltic Sea (Figure 1a); according to a recent study by Zhaka et al. (2024) the average diameter can be closer to 0.5 m.

The brash ice channel is typically described in two dimensions: the thickness of the brash ice pile and the width of the channel. The length is normally considered infinite. The old brash ice channel thickness can be profiled as thinnest at the centre and thickest close to the channel edges (Figure 1b).

Brash ice in the channel is traditionally understood as a granular material, a floating pile of ice blocks on seawater. Relate to its discrete nature, the brash ice can be considered as rigid ice blocks without fracture and inter-particle cohesion, as illustrated by the comparison of the model test and full-scale measure in terms of resistance (Mellor, 1980; Matala and Suominen, 2022, 2023a). When considering its continuum nature, the whole brash ice pile can be described by porosity, compressibility, internal friction angle and angle of repose (Matala and Gong, 2021). However, internal friction angle and angle of repose, important shear failure parameters, are difficult to measure on site and dependent on brash ice's mechanical response on a few variables, including tested volume, grain size and porosity, which are related to the brash ice discrete nature. Therefore, more attention should be paid to discretely numerically modelling brash ice.



(a)



(b)

**Figure 1: (a) Brash ice in a fairway channel in the Baltic Sea (Picture: Aker Arctic). (b) Vessel advancing in a brash ice channel and a transverse profile of a typical old brash ice channel in Baltic Sea. After Matala and Suominen (2023b) and Matala (2023).**

## 1.2 ICE CLASS SHIPS AND MODEL TEST

In the Baltic Sea, the winter navigation system is built up with an ice-going merchant fleet assisted by icebreakers. Finnish and Swedish authorities utilize ship classification based on the Finnish-Swedish ice class rules to determine the merchant ship's eligibility for icebreaker assistance. The ice-going merchant ships are typically designed to acquire an ice class, which ensures sufficient structural strength and power to operate in rule ice conditions.

Traditionally, the ice-going ships were designed to break level ice. As the current environmental standards focus on emission control, new ice-going bow designs have been developed for optimal over the full operational profile, and thus economical operation in open water and old brash ice channels.

Such ships could advance at relatively high speed in a brash ice channel. This challenges the current model tests to model open water friction accurately as the Reynolds similitude is not fulfilled, and the effect of hydrodynamics on the resistance cannot be neglected (Vance, 1974). However, in the industry, physical model tests are still considered the best method to determine a ship's ice performance before building the prototype. In recent years, numerical methods of simulating ships in ice have already started to transit from academic and research development to industrial applications (STAR-CCM+, a SIEMENS software). Significantly, special characters of channel brash ice can reduce the complexity of modelling brash ice numerically, which brings more confidence to build up an in-house numerical simulation of ships in brash ice by considering hydrodynamics. For instance, the full-scale observations reveal no significant deformation in brash ice fragments in an old, frequently operated brash ice channel. Thus, there is no significant breaking failure, and the brash ice mass is not submerged below the bow but mainly displaced to the sides.

## 1.3 SCOPE OF THIS REPORT

This report aimed to review previous studies on numerical simulating ships in a brash ice channel. The numerical methods of modelling brash ice were first reviewed. The review mainly focused on introducing the discrete element method for modelling brash ice. Other simulation methods used in brash ice modelling were also reviewed. Due to the important role of hydrodynamics, techniques of coupling the hydrodynamics to the DEM brash ice simulation were reviewed. Finally, the discussion was given on the possibility of using an open-source platform by considering implementing the model testing technique in the simulation.

Some papers related to ships in floe ice and ice ridge are also mentioned if necessary. For readers' interest, readers can refer to earlier review papers on broken ice interacting with ships (Xue et al., 2020; Li and Huang, 2022) and structures (Islam et al., 2021), covering not limited to brash ice but ice floes, ice ridge and pancake ice, etc.

## 2 NUMERICAL METHODS OF BRASH ICE

Numerical methods have recently been popularly applied in ice-ship (structure) interaction. Both numerical continuum, such as finite element method (FEM), and discontinuum methods, such as discrete element method (DEM), have been developed with mathematical deduction by considering the implementation of the computational calculation. In the ice-related field, the academia has led the development of the numerical methods. Based on understanding the physical nature of brash ice, particle-based numerical simulation method is a better option than continuum mechanics-based methods. The numerical methods have also developed from two dimensions to three dimensions. A good numerical method aims to have results closer to one series of model tests; the method itself should have physical solid meanings, and the material properties should be verified thoroughly (Tuhkuri and Polojärvi, 2018).

According to the authors' knowledge, DEM is a more suitable numerical method to simulate brash ice. The following sections first focus on the discrete element method applications in ice research and then briefly summarise other numerical method applications in brash ice.

### 2.1 DISCRETE ELEMENT METHOD (DEM)

The discrete element method is a particle-based method widely used in simulating granular materials in nature and industry, such as geophysics, chemical engineering, agricultural and food processing, and recently in ice mechanics. DEM has been promoted to model ice blocks by explicitly simulating Newtonian dynamics of interacting particles without a given assumed failure model or failure geometry of a pile of ice blocks. A good review of DEM applications on ice–structure interaction (ships and offshore structures) can be found in Tuhkuri and Polojärvi (2018), emphasising the importance of understanding the ice mechanics through DEM as the ice blocks can be considered as a discontinuous medium.

The DEM has been developed since Cundall and Strack (1979) published the cornerstone paper of DEM for granular assemblies. DEM can be divided into non-smooth DEM and smooth DEM related to implicit and explicit computational integration, which solves equations of rigid body motion. Suppose the equations of motion used to obtain the contact force and velocities are presented in the form of ordinary differential equations (ODE). In that case, usually, they are integrated with explicit time steps using small step sizes in smooth DEM. In comparison, non-smooth DEM solves the equations of motion for the entire contact network using an implicit time-integration algorithm (Servin et al., 2010).

The smooth DEM has been applied, referred to as the classical DEM formulation (Tuhkuri and Polojärvi, 2018): contact force models mimicking the effect of soft contacts and external forces acting on each block are solved on a given small time step. The equations of motion of rigid ice blocks using Newton's second law are solved explicitly in small time steps to determine accelerations. Then, the velocities and positions of each block are updated. Following this DEM simulation scheme, the Aalto University Ice Mechanics group developed an in-house DEM tool to study the mechanical behaviour of ice rubble

after Hopkins et al. (1991) and Hopkins (1992, 1998). The model-scale and full-scale ice rubble punch through test simulations verified the code and parameters (Polojärvi, 2013) in Figure 2. It is further applied to study the failure behaviour of an ice ridge, a linear pile of ice blocks with different widths, during different ship hull forms' penetration (Gong et al., 2017, 2018, 2019, a,b; Gong, 2021) in Figure 3 and Figure 4. The code has recently been updated to simulate ships in ice floe fields by considering the added mass and crack in the ice (Polojärvi et al., 2022; Polojärvi, 2023) in Figure 5 and Figure 6. The DEM simulations provide not only the ice resistance on the ship but also the distribution of the ice load on the hull (Polojärvi et al., 2021). The fragmentation and force chains were also observed in the simulations of the shear box tests of ice blocks (Prasanna and Polojärvi, 2023), giving more understanding of the mechanical behaviour of ice rubble under such loading conditions.

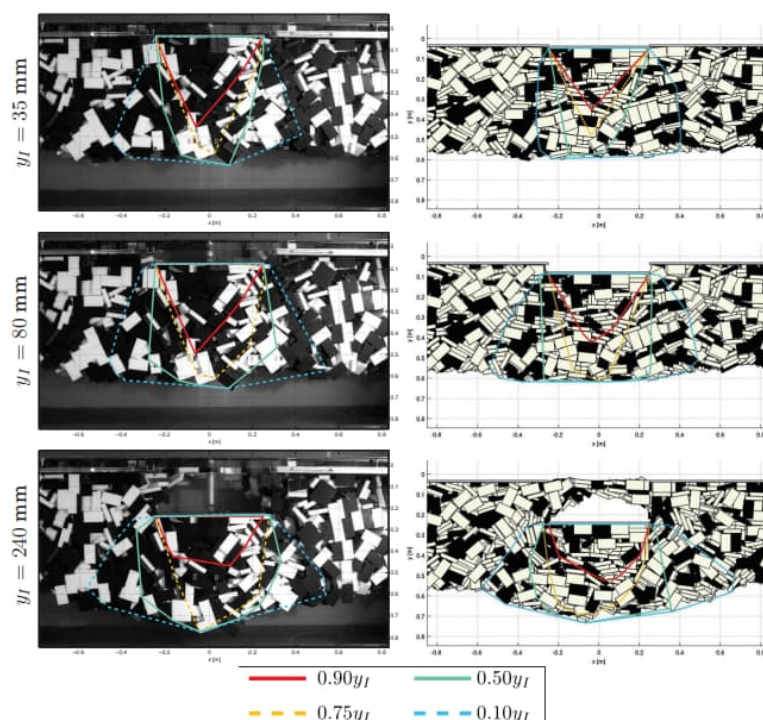


Figure 2: Laboratory scale (left) and virtual (right) punch through test on floating rubble. The colored lines describe the contours for rubble displacement. After Polojärvi (2013).

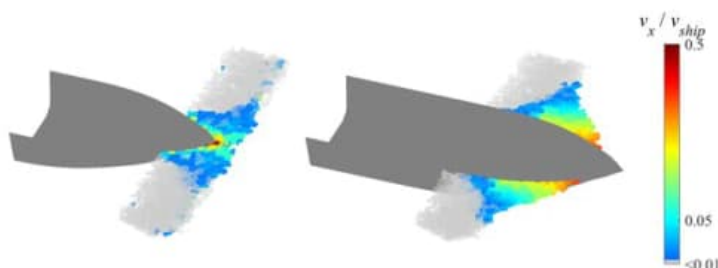


Figure 3: Ice blocks kinetic behaviour in an unconsolidated ice ridge passing by a ship, simulated by Aalto Ice Mechanics group in-house DEM after Gong et al. (2019a) and Gong (2021).

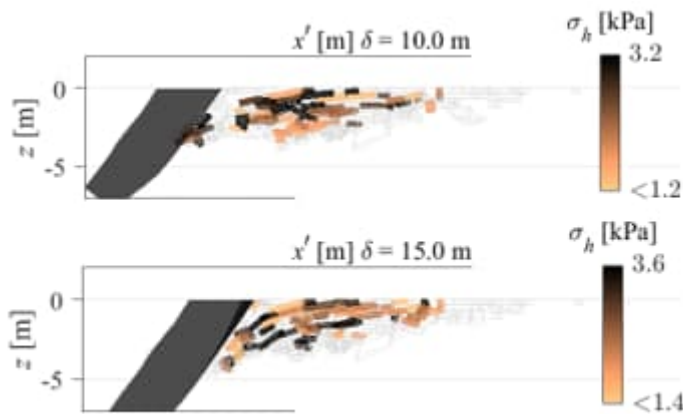


Figure 4: Force chains can be observed in ice ridge failure captured by DEM. After Gong et al. (2023).



Figure 5: Ship in an ice floe field simulation by using the Aalto Ice Mechanics group's in-house DEM code, after Polojärvi et al. (2021).

Aalto University Ice Mechanics group has also used the combined finite-discrete element method (FEM-DEM) to simulate level ice moving against offshore structures (Paavilainen, 2013; Ranta, 2018; Lilja, 2020; Lemström, 2022). The recently published work implemented the previous work into a three-dimensional FEM-DEM simulation by considering an ice sheet consisting of polyhedral rigid discrete elements joined by a lattice of Timoshenko beam elements (Polojärvi et al., 2022; Polojärvi, 2023). The current simulation model is only validated for low-speed ice-structure interaction processes by considering the drag force and ignoring other hydrodynamics effects.

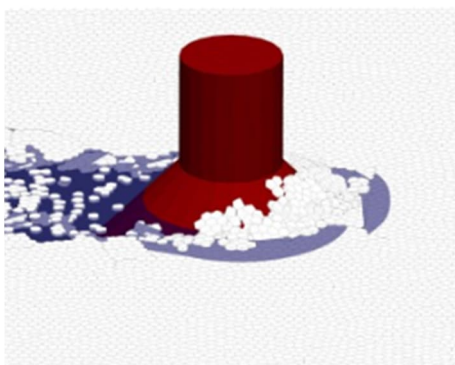


Figure 6: An ice-conical structure interaction simulation by Aalto Ice Mechanics group using in-house DEM after Polojärvi (2022).

Other DEM tools have also developed. The in-house code used by HSVA to simulate the ice ridge interaction by Hisette et al. (2017) and further application in ships in brash ice

(Prasanna, 2018). A summary of implicit, non-smooth and event-driven DEM simulations has also been used (Metrikin and Løset, 2013; Rabatel et al. 2015; van den Berg M, 2016; Daley et al., 2012) as stated in the review paper of Tuhkuri and Polojärvi (2018).

Based on the current development, as the model brash ice behaviour observed in model tests (Matala and Suominen, 2023b), only considering simulating the ice blocks, the smooth discrete element method of simulating rigid ice blocks would be ready for use. The further step is to couple computational fluid dynamics (CFD) into the simulation. The coupled DEM with CFD will be introduced in detail in Section 3.

## 2.2 OTHER NUMERICAL METHODS

### 2.2.1 OPEN DYNAMICS ENGINE

Ships in brash ice have also been simulated by using physics engines for serving the real-time ship navigation simulation by fast physics-related calculations prioritizing speed over accuracy (Tuhkuri and Polojärvi, 2018). Konno et al. have been developing simulation software using the Open Dynamics Engine, one of the physics engines (Konno, 2009; Konno and Yoshida, 2023). Figure 7 shows two snapshots of simulations of Japanese Bulk Carrier in a brash ice channel. The effect of the bow shape on the brash ice resistance was primarily deliberately studied based on the simulation results (Tokudome and Konno, 2023), which could be used for further comparison with other simulation methods.

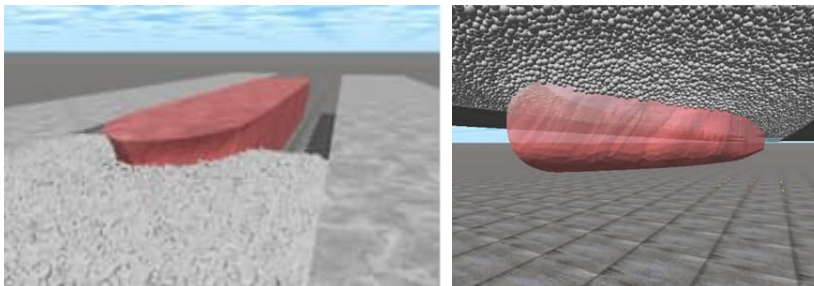


Figure 7: Snapshots of Japan Bulk Carrier navigation simulation in a brash ice channel. After Konno and Yoshida (2023) (left) and Tokudome and Konno (2023) (right).

### 2.2.2 FINITE ELEMENT METHOD COUPLED WITH ARBITRARY LAGRANGIAN EULERIAN

The finite element method has been employed in simulating ships in floe ice. Kim et al. (2013) investigated ship resistance in pack ice using LS-DYNA. Both the ship and pack ice were modelled as rigid bodies. Fluid flow used Eulerian formulation using dynamic viscosity and equations of state with a null material model. LS-DYNA does not include a full CFD solver; instead, hydrodynamics calculation uses a penalty method. Arbitrary Lagrangian Eulerian (ALE) method was applied to fully couple solutions of Lagrangian structures interacting with Eulerian fluids.

A similar simulation approach was applied in simulating a ship in floe ice later by Kim et al. (2019) in ABAQUS in Figure 8. The floe ice was modelled in a polygon shape without breakage and meshed by an extruded solid. The ice-sea water interaction was modelled

by the inbuilt coupling interface of ALE method. Although assumptions and simplifications restricted the simulation accuracy, it illustrated a complete case study in ABAQUS.

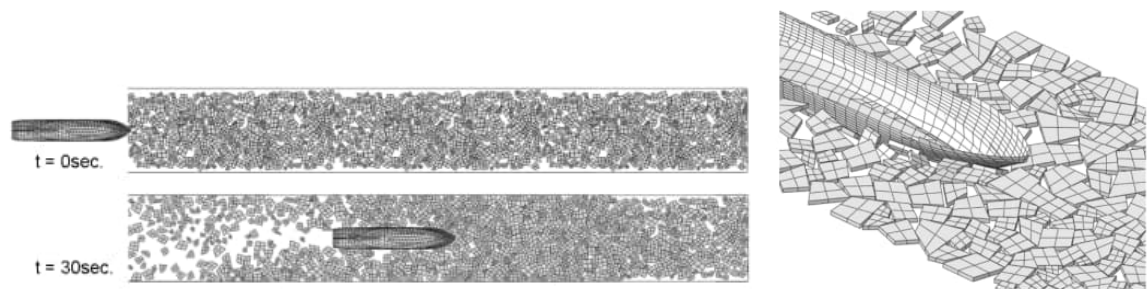


Figure 8: Snapshots of the simulation (left) and the hull and ice interaction (right). After Kim et al. (2019).

### 2.2.3 SMOOTHED PARTICLE HYDRODYNAMICS

Smoothed particle hydrodynamics (SPH) is a mesh-free simulation method that has become popular in recent years in the simulation of material under a large deformation, which the finite element method has difficulty handling in conventional solvers. Brash ice was recently modelled by SPH by Cabrera (2017) using open-source DualSPHysics. The scenario of a cylinder (SPH model) encountering brash ice in the channel was simulated, as shown in Figure 9. However, the author pointed out the complexity of upgrading the code by importing ships in an enlarged water domain.

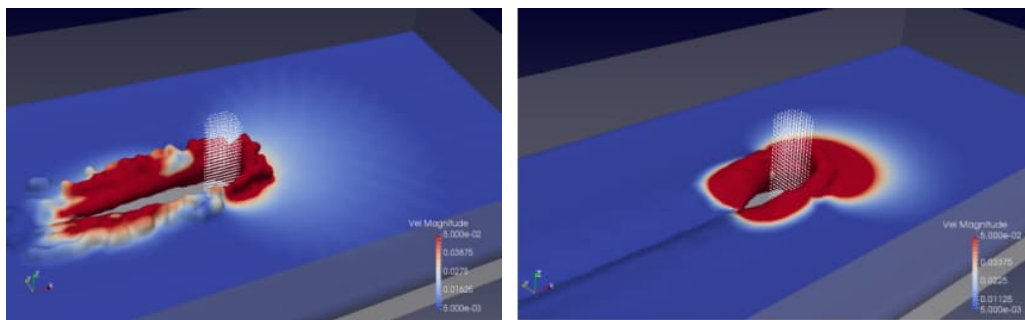


Figure 9: Cylinder in brash ice using SPH with different material parameters. After Cabrera (2017).

### 3 CFD-DEM NUMERICAL METHOD OF SHIP IN BRASH ICE

Based on the last section's review, DEM has been selected to simulate brash ice. As the current ship hull development and a wide range of ship types are required to be granted ice class, the effect of hydrodynamics on the ship performance in a brash ice channel should be considered deliberately. The simplified drag force calculated in DEM simulations might need to be more accurate when the ship advances at high speeds. Moreover, a significant bow wave might occur at high speeds which in turn changes the ice deformation processes at the bow. Thus, the following section reviews DEM modelling principles first and the methods of coupling CFD into DEM for brash ice channel simulation. According to the authors' knowledge, other simulation software applications have not yet been applied to ships in the brash ice channel. Recently, Luo et al. (2022) in Figure 10, Voutilainen (2022) in Figure 11 and Sun et al. (2023) in Figure 12 simulated ships in the brash ice channel in STAR-CCM+.

In the following sections, a review of the theoretical background of CFD-DEM will be given, starting with DEM-related techniques and then extending to CFD, emphasizing a discussion of the coupling scheme and further discussing the possibility of using MPI to reduce the computation time. Considering the practical issue, some techniques used by the open-source code YADE-CFD and Lethe will be introduced, mainly focusing on the possibility of shipping in the brash ice application.

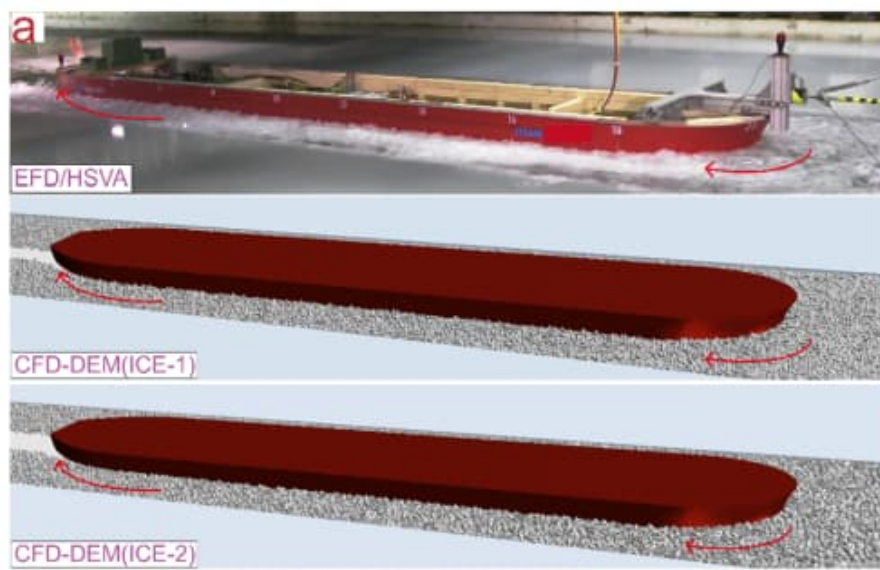


Figure 10: The view above the water of the experimental and numerical ship-ice interaction phenomenon. a. the side view of the interaction phenomena between ship hull and brash ice. After Luo, et al. (2022).



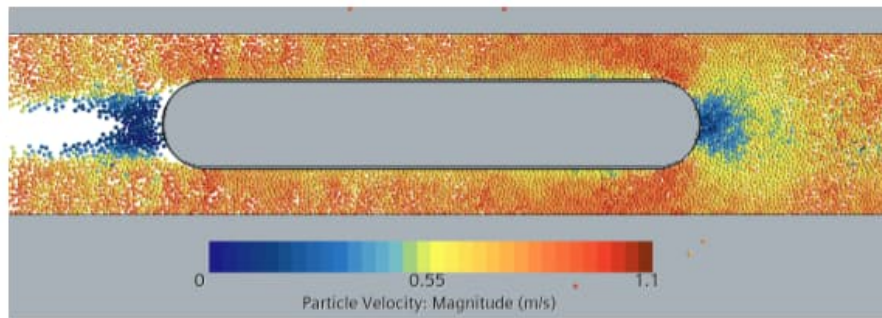


Figure 11: A ship hull in cylinder particles channel simulated in STAR-CCM+. After Voutilainen (2022).

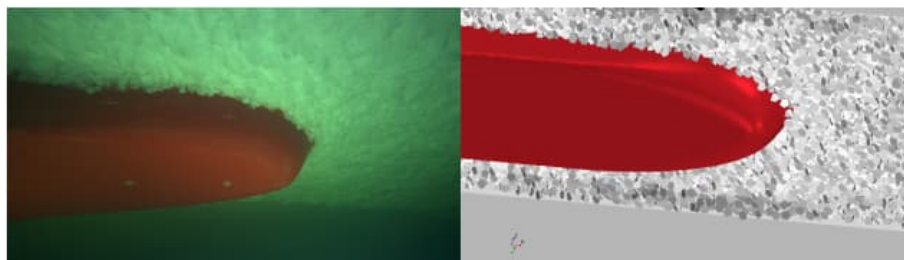


Figure 12: Comparison between the model tests and simulation of a 108k bulk carrier in 1A FSICR brash ice channel. After Sun et al. (2023).

### 3.1 TECHNIQUES OF DEM

DEM modelling considers material discretely by computing the kinetics of each particle or element confined by interaction through contacts. The particle shape model and contact detection should be modelled first, and then forces on the elements and the interaction among elements through contact forces should be added.

#### 3.1.1 GEOMETRY OF DISCRETE ELEMENTS

The shape of the discrete element was modelled from disc to (regular or irregular shape) polygon in two dimensions and sphere to polyhedron (convex or concave) in three dimensions. The element shape determines the contact search algorithm and further influences the contact force modelling. Modelling the discrete element shapes as close as possible to nature is recommended. The shape is important in determining the microscopic and macroscopic behaviours of the granular material (Ma et al., 2022). Especially considering the interaction between the discrete elements and the fluid, the shape of the discrete elements would pronouncedly influence the overall behaviour of the particle-flow system. Related to the ice study, the 3D DEM simulations of ships in ice floes (Polojärvi et al., 2021) have revealed that the shape of ice floes has a main role in determining the ice load magnitude on the ship, in addition to the ice thickness and size. Hence, a realistic geometry distribution of brash ice should be considered in the simulations.

Some full-scale data and model-scale data should be considered in the simulations. Matala and Gong (2021) studied model-scale brash ice shape from digital images from three ice sheets of model tests. The approach could be applied to obtain more

geometrical data on model-scale or full-scale brash ice. Recently, Zhaka et al. (2023) published macro-porosity and size distribution analyses from the brash ice channel field data in the Bay of Bothnia, Luleå port, Sweden, during winters 2020-21 and 2021-22. Other field data on ice block size in ridges can be found in Kulyakhtin, S. and Høyland, K., 2014. Where the probability distribution of the aspect ratio of the ice block size obtained from the field was used to create the 3D discrete elements for ships in ice ridge simulations.

Luo et al. (2022) used the STAR-CCM+ to simulate a bulk carrier in a brash ice channel. According to this study, the brash ice was simulated as so-called tetrahedral particles of isotropic and irregular polyhedral particles. In fact, they belong to the sphere-based particle model (Ma et al. 2022), meaning the object is created by assembling a certain number of spheres (refer to sub-sphere) to describe a particle with an arbitrary shape. The particle is usually rigid. The conventional spherical contact detection algorithm is used to detect sub-sphere contacts. The sum of forces and torques acting on each sub-sphere as resultant forces and torques are applied to the mass centre of the particle. So, the simulation can benefit from the high efficiency and strong robustness. Voutilainen (2023) also used the STAR-CCM+ to model the brash ice with cylindrical particles, reflecting the fresh-water ice blocks used in the model tests. The contact principle would be the same as earlier explained. Rigid discs were also used to simulate ice floes in STAR-CCM+ by Huang (2020).

For reference, polygon ice blocks have been used in simulating ice rubble (Polojärvi, 2013), ridges (Gong, 2021), and ice floes (Polojärvi et al., 2022).

### 3.1.2 CONTACT DETECTION

The contact detection methodology relates to the discrete element's geometry, which also determines the computational consumption of the DEM model. Ma et al. (2022) presented a detailed review of discrete element geometries and contact detection methods, categorised by the sphere-based particle models (multi-sphere model for rigid particles, bonded-sphere model for flexible and breakable ones, single spherical particle to represent the non-spherical particles), super-ellipsoid-based particle model (single-particle approach and composite-particle approach) and polyhedron-based model. Since the brash ice was found to be polyhedron shape with a certain roundness, the review of related contact detecting methods has been presented by Lu et al. (2015). Polojärvi (2022) presented the contact detection method of overlapping polyhedrons after Feng (2012), an energy-conserving contact interaction model for elastic-viscous-plastic articles where contact force is acting on the centroid of the overlap volume. This contact detection method eases the force application on the contacts. More techniques of contact modelling of non-spherical particles in DEM can refer to the recent review paper by Feng (2023).

### 3.1.3 PARTICLE MOTION EQUATION

In DEM, the discrete element is considered to be a rigid body. Newton's second law of motion determines particles' translational and rotational motions. Different authors

presented the equations with different named forces. Here taking the equation expressions from Ma et al. (2022):

$$m \frac{dv}{dt} = F_c + F_{coh} + F_{pf} + mg \quad [1]$$

$$I \frac{d\omega}{dt} = T_c + T_f \quad [2]$$

Where  $t$  is time,  $m$  and  $I$  are mass and inertia tensor.  $v$  and  $\omega$  are the linear velocity and angular velocity of the particle. The right-hand side of the equations is force- and torque-related terms.  $F_c$  and  $F_{coh}$  are contact force and cohesion force. Brash ice is considered without cohesion, therefore  $F_{coh} = 0$ .  $mg$  is gravity.  $F_{pf}$  is the interaction force between fluid and particle.  $T_c$  is contact torque and  $T_f$  is the torque caused by fluid.

### 3.1.4 CONTACT FORCE

According to Polojärvi (2022), the contact force  $F_c = F_n + F_t$ , divided into the normal force  $F_n$  and tangential force  $F_t$  based on the overlap volume techniques of contact detection model. The applied forces in the normal direction, including elastic (contact stiffness) force, viscous damping force, is limited by the plastic limit if the sum of elastic and damping force is over the plastic limit force depending on the rate of change of the overlap volume. And the applied forces in the tangential direction equal the sum of tangential contact stiffness force and tangential damping force limited by the coulomb friction.

Luo et al. (2022) used a modified variant of a non-linear spring-damped contact model to model brash ice, which was based on the Hertz-Mindlin contact model, an inbuilt non-linear contact model in the STAR-CCM+. The Hertz-Mindlin model is good at efficiently calculating sphere or disc-like discrete elements. Voutilainen (2023) simulated a cylinder hull in brash ice using linear spring model and Hertz-Mindlin model. It concluded that the simulated resistance was insensitive to the tested contact models used in STAR-CCM+. The detailed contact model's equations can be referred to STAR-CCM+ manuals (SIMENS STAR-CCM+ manual, 2023).

### 3.1.5 PARTICLE-FLUID INTERACTION FORCE

In Equation [1],  $F_{pf}$  covers drag force, lift force, pressure gradient force, virtual mass force, Basset force, etc. (Ma et al., 2022). The drag force is generally the largest and normally only considered in the simulations. One type of drag force equation concerning the sphere particles is formulated as

$$F_D = \frac{\pi d_p^3 \beta (u-v)}{6(1-\varepsilon)} \quad [3]$$

where  $d_p$  is the diameter of the volume equivalent sphere,  $\beta$  is the interphase exchange coefficient,  $u$  is fluid speed.  $\varepsilon$  is the void fraction or volume fraction defined as the proportion of fluid accounted for the flow and pressure effects from the neighbouring particles. For a loose granular system,  $\varepsilon = 0$ ; for dense granular systems,  $0 < \varepsilon < 1$ . For non-spherical particles, drag force is more difficult to model accurately as both the

irregular shape and orientation can significantly affect the flow field and particle-flow interaction. A coefficient was introduced to correct the inaccuracy based on the drag force formula mentioned above. For more details, refer to Ma et al. (2022).

The YADE CFD-DEM open-source code used two methods to model the hydrodynamics of particles and flow: point force coupling and volume averaged coupling. In both approaches, the particle scale's flow is not resolved, and analytical/empirical hydrodynamic force models are used to describe the particle-flow interactions. The particle size must be smaller than the fluid cell size for accurate resolution of the particle volume fraction and hydrodynamic forces on the fluid grid (YADE, 2023).  $F_D$  is a variant of Equation [3]. The detailed expression is presented in YADE (2023).

Polojärvi (2022) used the classic pressure drag load as drag force, formulated as

$$F_d = 0.5\rho_w c_d A_d v^2 \quad [4]$$

where  $\rho_w$  is water density,  $c_d$  is drag coefficient,  $A_d$  is the cross-section area of the body, and  $v$  is the relative velocity between a fluid and a body. Huang, et al. (2021) used a variant of Equation [4] with a different drag coefficient from Polojärvi (2022). Compared to  $F_D$ ,  $F_d$  does not consider the particle-flow interaction.

Pressure gradient force is typically considered as buoyancy governed by the Archimedes principle as  $F_b = \rho_w g V$ , where  $V$  is the particle's volume. Virtual mass force is related to the fluctuation of particle velocity. In principle, added mass and inertia when integrating their equations of motion (Polojärvi, 2022).

In reviewed brash ice-ship simulations, lift force and Basset force were not applied in the brash ice simulations. The necessities of these two forces shall be investigated later.

## 3.2 THEORY BACKGROUND OF CFD

In the particle-flow system, CFD solvers generally discretise the computational domains by a finite volume or cell and solve the nonlinear flow equations with the iterative method. The DEM solver is on the other hand to solve the equations at particle scale. It requires an interface for coupling with CFD solvers. For now, three coupling strategies exist between the fluid solver and DEM regarding the ratio of CFD cell size to particle diameter. Based on the size ratio, over 3 is named the unresolved CFD-DEM model, below 1/10 of the particle diameter is the resolved model, and in between is the semi-resolved CFD-DEM model. According to the description of Yade CFD-DEM and Lethe CFD-DEM and the practical of the physical nature of the brash ice in the water, the unsolved CFD-DEM model is suitable for modelling ship in brash ice that CFD cell contains several solid particles. The Navier-Stokes equations of particle-fluid coupling are solved based on the local average using the volume or void fraction. The continuity equation and momentum conservation equation are formulated as

$$\frac{\partial}{\partial t}(\varepsilon\rho_f) + \frac{\partial}{\partial x_j}(\varepsilon\rho_f u_j) = 0 \quad [5]$$

$$\frac{\partial}{\partial t}(\varepsilon \rho_f u_i) + \frac{\partial}{\partial x_j}(\varepsilon \rho_f u_j u_i) = -\frac{\partial p}{\partial x_i} + \frac{\partial}{\partial x_i} \left[ \varepsilon u_f \left( \frac{\partial u_i}{\partial x_j} + \frac{\partial u_j}{\partial x_i} \right) \right] + F_s \quad [6]$$

Where  $u$  is the fluid velocity,  $p$  is the fluid pressure,  $x$  denotes the coordinates,  $\varepsilon$  is void fraction,  $\rho_f$  is the fluid density, and  $F_s$  is the source terms representing the forces due to particle and fluid interaction.

The second term on the right-hand side of the momentum conservation equation is related to the stress tensor of the fluid, and  $F_s$  generally covers Particle-fluid interaction forces, including drag force, added mass force and buoyance. STAR-CCM+ uses such a momentum equation. Lethe uses two Volume Average Navier-Stokes (VANS) equation models to represent the fluid phase. Model A considers pressure and viscous shear stress in the solid and fluid phases, while Model B is only in the fluid phase. According to Geitani et al. (2023), models A and B are mathematically equivalent; they result in different instantaneous physical behavior. In the simulation of fluidized beds, model A is more stable and results in less stiffness of the system being solved.

$$\frac{\partial}{\partial t}(\varepsilon \rho_f u_i) + \frac{\partial}{\partial x_j}(\varepsilon \rho_f u_j u_i) = -\varepsilon \frac{\partial p}{\partial x_i} + \varepsilon \frac{\partial}{\partial x_i} \tau - F_{pf}^A \quad [7]$$

$$\frac{\partial}{\partial t}(\varepsilon \rho_f u_i) + \frac{\partial}{\partial x_j}(\varepsilon \rho_f u_j u_i) = -\frac{\partial p}{\partial x_i} + \frac{\partial}{\partial x_i} \tau - F_{pf}^B \quad [8]$$

Where  $\tau$  is shear stress,  $F_{pf}^A$  and  $F_{pf}^B$  are the source terms representing the forces applied back in the fluid due to the interaction with the particle's for Model A and B, respectively. For Model A, pressure and shear stress terms are partially in the particle's phase,  $F_{pf}^A$  is formulated as  $F_{pf}^A = \frac{1}{V_\Omega} \sum_i^{n_p} F_{pf,i} - F_{\nabla p,i} - F_{\nabla \tau,i}$ . For Model B, the pressure and shear stress are totally in the fluid,  $F_{pf}^B = \frac{1}{V_\Omega} (F_{pf,i})$ , where  $n_p$  is the number of particles inside the cell  $\Omega$  with volume  $V_\Omega$ . For more details, please refer to Lethe (2023).

YADE assumes incompressible flow, the equation is expressed as

$$\frac{\partial}{\partial t}(\varepsilon u_i) + \frac{\partial}{\partial x_j}(\varepsilon u_j u_i) = -\frac{\partial p}{\rho_f \partial x_i} + \varepsilon \frac{\partial}{\partial x_i} \tau + F_s \quad [9]$$

Where  $F_s = S_u + \varepsilon g - K(u - v)$ ,  $K$  is the particle drag force parameter,  $u$  and  $v$  are the fluid and particle velocities respectively.  $S_u$  denotes the explicit source term consisting the effect of other hydrodynamic forces such as the Archimedes/ambient force, added mass force etc. For more details, please refer to YADE (2023).

Depending on the simulation application, the momentum conservation equation can be written in different forms regarding fluid density and void fraction. The particle-fluid interaction forces are also presented in different forms accordingly. For an open-source platform, the end users have the possibility to change the force formulas.

### 3.3 COUPLING SCHEME BETWEEN CFD AND DEM

Depending on the simulation platforms, either starting with DEM, CFD, or both simultaneously to initialise the program. For example, if starting with DEM, based on the

equations, the DEM can first provide information about particles, such as the velocity and position of the particles in one fluid cell. This information inputs to the CFD solvers, contributing to the right-hand side term of particle-fluid forces, which can be calculated based on the sum of the forces on the particles divided by the cell's volume to obtain the average force to the fluid cell. Subsequently, the fluid flow can be calculated and added to the motion of particles of the cell for the next time step to obtain the resultant forces induced by fluid into DEM. This process requires calculating void or volume fraction. Traditionally, the void fraction scheme is formulated as one minus the sum of the particle's volume considered in the CFD cell's volume. However, this simple scheme would result in the accuracy of the fraction value, which determines the accuracy of the calculation. It introduces spatial weight to accurately represent the particle volume fraction inside the cell. In YADE, Gaussian weight is applied (YADE, 2023) to interpolate and average the Eulerian and Lagrangian quantities of the equations. In Lethé, the void fraction is calculated by the particle centroid method due to its simplicity (Geitani, 2023; Lethé, 2023). Another method of volume fraction used in STAR-CCM+ was introduced in Voutilainen (2022). Other weight methods were introduced based on different particle shapes by Ma et al. (2022).

Most recently developed open-source Lethé CFD-DEM (Geitani et al., 2023) aims to solve the computational expenses from coupling both necessitates the calculation of the void fraction and the solid-fluid forces. A monolithic finite element CFD-DEM solver supporting dynamically load-balanced parallelization has been developed to allow more stable, accurate and time efficient simulations. The figure below shows the Lethé CFD-DEM coupling scheme after Geitani et al. (2023). It restricts the coupling frequency. For example, the coupling frequency is defined as the ratio of CFD's time step and DEM's 100. It means that the coupling that happens in the DEM time step should be  $10^{-5}$  when the CFD time step is  $10^{-3}$ , for example. The cell volume should also be at least 10 times greater than the particle volume.

The process shown in Figure 13 presents two-way coupling, meaning the fluid phase affects the ice particles, and the motion of the ice particles also affects the fluid. In comparison, the one-way coupling is used to calculate fluid flow by CFD and its effect on the particles. However, the motion of the particles will not affect the fluid, so the interaction between ice particles and fluid is neglected. Luo et al. (2022) stated that the two-way coupling can more accurately simulate the brash ice near the bow. This is the reason for introducing two-way coupling CFD-DEM. Although the computational cost is much higher, parallel calculation makes it worth trying to establish two-way coupling.

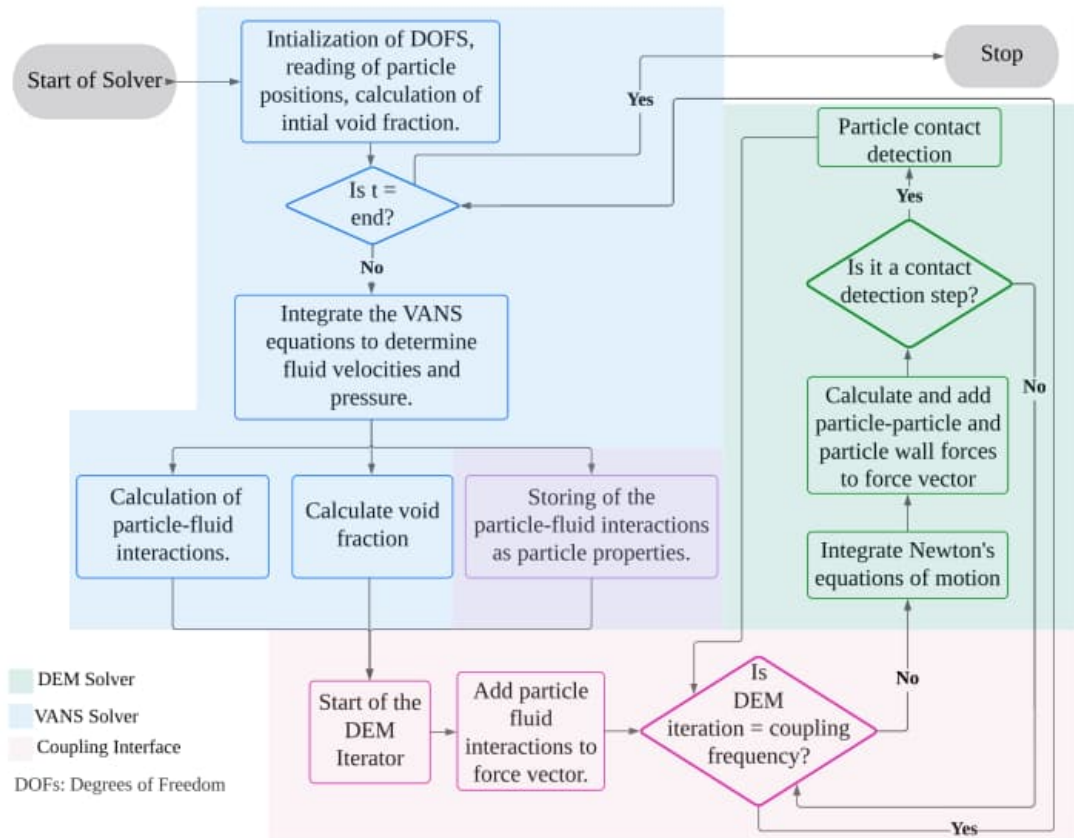


Figure 13: Lethe CFD-DEM coupling scheme. After Geitani et al. (2023).

## 4 DISCUSSION

As presented in the report, YADE and Lethe are two open-source codes which can potentially be used to model ship passing through brash ice channel. It is also possible to continue to develop the Aalto University Ice Mechanics group's in-house code by adding the CFD coupling method. Both approaches are plausible as the basic CFD-DEM frame has been built.

The code-developing target should have solid physical proof with a relatively reasonable computational cost. When using the open-source platform, the disc or sphere DEM particles can be used initially. More effort should be made to select suitable contact force models and contact detection techniques. The ship's model can be meshed as volume and simulated as discrete elements, such as output from SolidWorks and meshed in GMSH. The momentum equation should be chosen according to the ship operating over 5 knots in the brash ice channel environment. The particle-fluid interaction force models shall also be selected accordingly.

The code stability shall also be debugged as the simulation will use larger time steps for longer simulations. The number of particles in the cell volume should be selected according to the limitation of the code, such as 10 for Lethe and 3 for YADE. The cells of the fluid field around the ship hull shall also be meshed by considering the brash ice movement around the hull, especially the bow area.

The first version of the simulation could be compared with the work done by Voutilainen (2022) and the available model test results. Verifications could also be done by other tests. Particular attention should be paid to comparing the brash ice kinetic behaviour between the simulations and model tests, such as the brash ice movement around the bow. The ship model's speed can be set up as constant. Further work shall consider replicating the current model test procedures and comparison with full-scale data.

The DEM-CFD numerical tool has an important role in arctic technology. From the ship's design perspective, besides the simulated brash ice resistance output, the local ice loads on the hull can also be obtained, as has been proven by Polojärvi et al. (2021). Such results are significant for the structural design on the ice belt, as the model test results could not be entirely representative. The effect of hull forms on the brash ice resistance by considering the hydrodynamics is also significant for the future hull form design. From the ice mechanics' perspective, the simulation could be used to understand the brash ice failure behaviour under the ship's passage by studying the effect of hydrodynamics on the brash ice resistance and the force transmission in the brash ice channel.

Overall, a DEM-CFD numerical tool could bring an alternative to evaluate ship channel resistance besides model-test-based determination for classifying ship ice class. For the Class Society, understanding the numerical calculation principle is important for making criteria to validate simulation results. Criteria could be to standardize, for instance, brash ice shape (Section 3.1.1), contact force model (Section 3.1.4, 3.1.5), and coupling method (Section 3.2, 3.3) with important material parameters and other computational inputs.



## 5 CONCLUSION

This report reviewed the current numerical methods used in simulating ships in a brash ice channel. The coupled DEM and CFD method is a suitable approach for the application by modelling brash ice in DEM and water in CFD when considering a ship operating at high speed. The theories of DEM and CFD and coupling methods were introduced. Two potential open-source platforms could be considered for starting to build up a DEM-CFD numerical tool for calculating the ice resistance of ships in a brash ice channel. Such a tool could benefit from predicting the ice performance of any ship hull forms in addition to the model tests. The ice loads obtained from the simulations can also provide essential information for the ice belt structure design.

## **6 ACKNOWLEDGEMENT**

The authors would like to thank the technical support of Dr. Malith Prasanna from the Aalto University Ice Mechanics Group of Marine and Arctic Technology. The authors would also like to acknowledge the financial support from the Finnish-Swedish Winter Navigation Research Board through project W23-6 CresSi and Aker Arctic Technology Inc.

## REFERENCES

- Cabrera, M.I., 2017. Smoothed particle hydrodynamics modeling of brash ice. University of Rostock, Rostock.
- Cundall, P.A., Strack, O.D., 1979. A discrete numerical model for granular assemblies. *Geotechnique*, 29(1), pp.47-65.
- Daley, C., Alawneh, S., Peters, D., Quinton, B., Colbourne, B., 2012. GPU modeling of ship operations in pack ice. In International Conference and Exhibition on Performance of Ships and Structures in Ice, ICETECH 2012, Banff, Alberta, Canada. Alexandria, VA.
- Feng, Y.T., Han, K., Owen, D., 2012. Energy-conserving contact interaction models for arbitrarily shaped discrete elements. *Computer Methods in Applied Mechanics and Engineering*, 205–208, pp. 169-177.
- Feng, Y.T., 2023. Thirty years of developments in contact modelling of non-spherical particles in DEM: a selective review. *Acta Mechanica Sinica*, 39(1), p.722343.
- Geitani, T, Golshan, S., Blais, B., 2023. A high-order stabilized solver for the volume averaged Navier-Stokes equations. *International Journal for Numerical Methods in Fluids*, 95:1011–1033.
- Gong, H., Polojärvi, A., Tuhkuri, J., 2017. Preliminary 3D DEM Simulations on Ridge Keel Resistance on Ships. In Proceedings of the 24th International Conference on Port and Ocean Engineering under Arctic Conditions, POAC'17: Busan, Korea.
- Gong, H., Polojärvi, A., Tuhkuri, J., 2018. 3D DEM Study on the Effect of Ridge Keel Width on Rubble Resistance on Ships. In ASME 2018 37th International Conference on Ocean, Offshore and Arctic Engineering.
- Gong, H., Polojärvi, A., Tuhkuri, J., 2019a. Discrete element simulation of the resistance of a ship in unconsolidated ridges, *Cold Regions Science and Technology*, p. 102855.
- Gong, H., Polojärvi, A., Tuhkuri, J., 2019b. The effect of ship bow shape on ridge resistance in a narrow ridge. In Proceedings of the 25th International Conference on Port and Ocean Engineering under Arctic Conditions, POAC'19: Delft, The Netherlands.
- Gong, H., 2021. Discrete-element modelling of ship interaction with unconsolidated ice ridges: ridge resistance and failure behaviour. Doctoral thesis, Aalto University.
- Gong, H., Polojärvi, A., Tuhkuri, J., 2023. Velocity field and force distribution in an unconsolidated ice ridge penetrated by a ship. In International Conference on Port and Ocean Engineering under Arctic Conditions, Glasgow, UK.
- Hisette, Q., Alekseev, A., Seidel, J., 2017. Discrete element simulation of ship breaking through ice ridges, In Proceedings of the 27th International Ocean and Polar Engineering Conference.
- Huang, L., Jukka Tuhkuri, J., Igrac, B., Li, M., Stagonas, D., Toffoli, A., Cardiff, P., Thomas, G., 2020. Ship resistance when operating in floating ice floes: A combined CFD&DEM approach. *Marine Structures*, 74, p.102817.
- Huang, L., Li, M., Romu, T., Dolatshah, A., Thomas, G., 2021. Simulation of a ship operating in an open-water ice channel. *Ships and Offshore Structures*, 16(4), pp.353-362.
- Hopkins, M.A., Hibler III, W.D., Flato, G.M., 1991. On the numerical simulation of the sea ice ridging process. *Journal of Geophysical Research: Oceans*, 96(C3), pp.4809-4820.
- Hopkins, M.A., 1992. Numerical Simulation of Systems of Multitudinous Polygonal Blocks. USARREL Report CR 99-22. US Army Cold Regions Research and Engineering Laboratory.
- Hopkins, M.A., 1998. Four stages of pressure ridging. *Journal of Geophysical Research: Oceans*, 103(C10), pp.21883-21891.

- Islam, M., Mills, J., Gash, R., Pearson, W., 2021. A literature survey of broken ice-structure interaction modelling methods for ships and offshore platforms. *Ocean Engineering*, 221, p.108527.
- Kulyakhtin, S., Høyland, K., 2014. Distribution of ice block sizes in sails of pressure ice ridges. In *Proceedings of the 22nd IAHR International Symposium on Ice*, pp. 235-240.
- Lemström I., 2022. Ice-structure interaction in shallow water - A study based on laboratory-scale experiments and discrete element simulations. Doctoral Thesis. Aalto University.
- Lethe, 2023. [https://lethe-cfd.github.io/lethe/theory/unresolved\\_cfd-dem/unresolved\\_cfd-dem.html](https://lethe-cfd.github.io/lethe/theory/unresolved_cfd-dem/unresolved_cfd-dem.html).
- Li, F., Huang, L., 2022. A review of computational simulation methods for a ship advancing in broken ice. *Journal of Marine Science and Engineering*, 10(2), p.165.
- Lilja, V.P., 2020. Finite-discrete element modelling of sea ice sheet elasticity, sea ice sheet fracture, and ice-structure interaction-A three-dimensional, lattice-based approach. Doctoral Thesis. Aalto University.
- Lu, G., Third, J.R., Müller, C.R., 2015. Discrete element models for non-spherical particle systems: From theoretical developments to applications. *Chemical Engineering Science*, 127, pp.425-465.
- Luo, W., Jiang, D., Wu, T., Guo, C., Wang, C., Deng, R. and Dai, S., 2020. Numerical simulation of an ice-strengthened bulk carrier in brash ice channel. *Ocean Engineering*, 196, p.106830.
- Kim, M., Lee, S., Lee, W., Wang, J., 2013. Numerical and experimental investigation of the resistance performance of an icebreaking cargo vessel in pack ice conditions. *International Journal of Naval Architecture and Ocean Engineering*, 5(1), pp. 116-131.
- Kim, J.H., Kim, Y., Kim, H.S., Jeong, S.Y., 2019. Numerical simulation of ice impacts on ship hulls in broken ice fields. *Ocean Engineering*, 182, pp.211-221.
- Konno A., 2009. Resistance evaluation of ship navigation in brash ice channels with physically based modeling. In *Proceedings of the 20th International Conference on Port and Ocean Engineering under Arctic Conditions, POAC'09*. Luleå, Sweden.
- Konno, A., Yoshida Y., 2023. Investigation of relationship between brash ice conditions and ship resistance, In *Proceedings of the 27th International Conference on Port and Ocean Engineering under Arctic Conditions*.
- Ma, H., Zhou, L., Liu, Z., Chen, M., Xia, X., Zhao, Y., 2022. A review of recent development for the CFD-DEM investigations of non-spherical particles. *Powder Technology*, 412, 117972.
- Matala, 2023. Verification of vessel resistance in old brash ice channels through model scale tests. Doctoral Thesis. Aalto University.
- Matala, R., Gong, H., 2021. The effect of ice fragment shape on model-scale brash ice material properties for ship model testing. In *Proceedings of the 26th International Conference on Port and Ocean Engineering under Arctic Conditions*, pp. 14-18.
- Matala, R., Suominen, M., 2022. Investigation of vessel resistance in model scale brash ice channels and comparison to full scale tests. *Cold Regions Science and Technology*, 201, p.103617.
- Matala, R., Suominen, M., 2023a. Scaling principles for model testing in old brash ice channel. *Cold Regions Science and Technology*, 210, p.103857.
- Matala, R., Suominen, M., 2023b. Impact of new bow shapes on FSICR power requirements. In *Proceedings of International Conference on Offshore Mechanics and Arctic Engineering (Vol. 86885, p. V006T07A008)*. ASME.

- Mellor, M., 1980., Ship resistance in thick brash ice. *Cold Regions Science and Technology* 3 (4), 305–321.
- Metrikin I., Løset S., 2013. Nonsmooth 3D discrete element simulation of a drillship in discontinuous ice. In *Proceedings of the 22nd International Conference on Port and Ocean Engineering under Arctic Conditions, POAC'13*. Espoo, Finland.
- Paavilainen, J., 2013. Factors affecting ice loads during the rubbing process using a 2D FEM-DEM Approach. Doctoral Thesis. Aalto University.
- Polojärvi, A., 2013. Sea ice ridge keel punch through experiments: model experiments and numerical modeling with discrete and combined finite-discrete element methods. Doctoral thesis.
- Polojärvi, A., Gong, H., Tuhkuri, J., 2021, June. Comparison of full-scale and DEM simulation data on ice loads due to floe fields on a ship hull. In *Proceedings of the 26th International Conference on Port and Ocean Engineering under Arctic Conditions, Moscow, Russia*, pp. 14-18.
- Polojärvi, A., 2022. Numerical model for a failure process of an ice sheet. *Computers & Structures*, 269, p.106828.
- Polojärvi, A., 2023. Three-dimensional numerical model for ice-structure interaction process. In *Proceedings of the 27th International Conference on Port and Ocean Engineering under Arctic Conditions, Glasgow, UK*.
- Prasanna, M., 2018. Numerical Simulation of Brash Ice, Master Thesis. Rostock, Germany.
- Prasanna, M. and Polojärvi, A., 2023. Ice block breakage within deforming ice rubble. In *International Conference on Port and Ocean Engineering under Arctic Conditions, Glasgow, UK*.
- Rabatel M., Labbé S., Weiss J., 2015. Dynamics of an assembly of rigid ice floes. *J. Geophys. Res.: Oceans* 120, 5887–5909.
- Ranta, J., 2018. Discrete element modeling of ice failure against an inclined structure—statistical analyses of peak loads and the failure process. Doctoral Thesis. Aalto University.
- Servin, M., Wang, D., Lacoursière, C. and Bodin, K., 2010. Examining the smooth and nonsmooth discrete element approaches to granular matter. *International Journal for Numerical Methods in Engineering*, 00:1–25.
- SIMENS STAR-CCM+ manual, 2023.  
<https://docs.sw.siemens.com/documentation/external/PL20200805113346338/en-US/userManual/userguide/html/index.html>.
- Sun, H., Ni, X., Zhang, Y., Chen, K. and Ni, B., 2023. A Numerical Prediction of the Resistance of Bulk Carriers in Brash Ice Channels. *Journal of Marine Science and Engineering*, 11(7), p.1425.
- Tokudome, T., Konno, A., 2023. Ship bow shape effects on brash ice channel resistance. *Cold Regions Science and Technology*, 206, p.103747.
- Tuhkuri, J., Polojärvi, A., 2018. A review of discrete element simulation of ice–structure interaction. *Philosophical Transactions of the Royal Society A: Mathematical, Physical and Engineering Sciences*, 376(2129), p.20170335.
- van den Berg M., 2016. A 3-D random lattice model of sea ice. In *Proc. of the Arctic Technology Conf. 2016, St. John's, Canada (ATC)*. Houston, TX.
- Vance, G., 1974. A modeling system for vessels in ice. Doctoral thesis. University of Rhode Island.
- Voutilainen, J., 2023. Computational analysis of brash ice and flow field around simplified body. Master thesis. Aalto University.

Xue, Y., Liu, R., Li, Z. and Han, D., 2020. A review for numerical simulation methods of ship–ice interaction. *Ocean Engineering*, 215, p.107853.

YADE, 2023a. <https://yade-dev.gitlab.io/trunk/FoamCoupling.html>

Zhaka, V., Bridges, R., Riska, K., Cwirzen, A., 2024. Brash ice macroporosity and piece size distribution in ship channels. *Cold Regions Science and Technology*, 217, 104047.